



HAL
open science

Photocatalytic degradation of atrazine by an N-doped TiO₂/polymer composite: catalytic efficiency and toxicity evaluation

Wanda Navarra, Olga Sacco, Christophe Daniel, Vincenzo Venditto, Vincenzo Vaiano, Davide A.L. Vignati, Clément Bojic, Giovanni Libralato, Giusy Lofrano, Maurizio Carotenuto

► To cite this version:

Wanda Navarra, Olga Sacco, Christophe Daniel, Vincenzo Venditto, Vincenzo Vaiano, et al.. Photocatalytic degradation of atrazine by an N-doped TiO₂/polymer composite: catalytic efficiency and toxicity evaluation. *Journal of Environmental Chemical Engineering*, 2022, 10 (4), pp.108167. 10.1016/j.jece.2022.108167 . hal-03715582

HAL Id: hal-03715582

<https://hal.univ-lorraine.fr/hal-03715582>

Submitted on 6 Jul 2022

HAL is a multi-disciplinary open access archive for the deposit and dissemination of scientific research documents, whether they are published or not. The documents may come from teaching and research institutions in France or abroad, or from public or private research centers.

L'archive ouverte pluridisciplinaire **HAL**, est destinée au dépôt et à la diffusion de documents scientifiques de niveau recherche, publiés ou non, émanant des établissements d'enseignement et de recherche français ou étrangers, des laboratoires publics ou privés.

Photocatalytic degradation of atrazine by an N-doped TiO₂/polymer composite: catalytic efficiency and toxicity evaluation

Wanda Navarra^{1*}, Olga Sacco¹, Christophe Daniel¹, Vincenzo Venditto¹, Vincenzo Vaiano², Davide Anselmo Luigi Vignati³, Clément Bojic³, Giovanni Libralato⁴, Giusy Lofrano^{5*}, Maurizio Carotenuto¹

¹ Department of Chemistry and Biology “A. Zambelli”, and INSTM Research Unit, University of Salerno, Via Giovanni Paolo II, 132, 84084 Fisciano (SA), Italy

² Department of Industrial Engineering, University of Salerno, Via Giovanni Paolo II 132, 84084 Fisciano (SA), Italy

³ Université de Lorraine, CNRS, LIEC, F-57000 Metz, France.

⁴ Department of Biology, University of Naples Federico II, Via Cinthia 21, 80126, Naples, Italy.

⁵ Department of Movement, Health and Human Sciences, University of Rome Foro Italico, Piazza Lauro De Bosis, 15, 00135 Rome (Italy).

*Corresponding authors:

Tel: +39/089969362

E-mail: wnavarra@unisa.it

Tel: +39/ 347 9060670

E-mail: giusy.lofrano@uniroma4.it

Abstract

Monolithic composite aerogel based on N-doped TiO₂ (NdT) photocatalyst dispersed into syndiotactic polystyrene (sPS) matrix was used for atrazine (ATZ) degradation under ultra-violet (UV) and visible light (Vis) irradiation. sPS/NdT composite aerogel, with a polymer/photocatalyst 90/10 weight ratio, was achieved by super critical CO₂ extraction of chloroform from the relative

sPS/NdT gel. Testing of the sPS/NdT photocatalytic activity was performed by using initial ATZ concentration of 0.1 mg/L and a sPS/NdT composite in monolithic aerogel form. ATZ removal was equal to 47 and 25 % under UV or Vis light, respectively, after 180 min of irradiation. The efficiency of the photocatalytic process was also investigated by monitoring the ecotoxicity of the treated water to *Aliivibrio fischeri*, *Raphidocelis subcapitata*, and *Daphnia magna*. The results indicated that, for both UV and Vis irradiation, even for high ATZ removal efficiency (i.e., UV treatment), the toxicity of process effluent is greater than the initial one, most likely because of the generation of toxic by-products. The UV treatment was effective only after 72 h when the solution appeared not toxic to *D. magna* and presented a very low effect to *R. subcapitata*. On the other hand, under Vis light irradiation, a very high level of toxicity was still detected after 72h of treatment time. Toxicity tests are confirmed as an indispensable tool for a correct assessment of the environmental impact of water treatment processes.

Keywords

Atrazine; Polymeric aerogel; N-doped TiO₂; Photocatalysis; Ecotoxicity.

1. Introduction

Atrazine (2-chloro-4-ethyl-amino-6-isopropylamino-1,3,5-triazine) is currently the second most used chemical weeds control agent in the world, due to its low cost and high effectiveness [1]. The global market is expected to register an increase of growth rate of 6 % from 2019 to 2024, reaching a turnover of 2.58 USD billion by the end of 2024 [2].

Despite its low water solubility, ATZ is highly persistent in soils (half-life from 60 to > 100 days) and can potentially contaminate surface and groundwater [3]. Toxicological studies classified atrazine genotoxic [4] and cytotoxic [5], possible teratogenic [6], carcinogenic [7], and endocrine disrupter [8,9], showing that the presence of atrazine into the environment can be dangerous for

biota and human health [10]. As a result, ATZ was classified as a priority substance by the European Parliament [11,12] and banned in the European Union in 2003 [13]. However, its use is still authorized by other agencies, such as the United States Environmental Protection Agency [14] and in developing countries, such as China and India [15,16]. Atrazine is directly applied to the soil surface or sprayed on weeds and through the runoff of water enters the aquifer, where its concentrations range from 3.90 to 15000 ng/L [17,18]. Other hot spots of atrazine contaminations are wastewater treatment plants (WWTPs) where atrazine can be present as result of the cleaning of containers used to store the pesticides and application equipment in agriculture and manufacturing plants. Most WWTPs fail to completely degrade triazines by releasing them with effluents into receiving nearby water bodies. Concentrations ranging from 49 to 870 ng/L have been detected in USA WWTPs effluents [19,20].

Various treatments have been attempted to degrade atrazine, including adsorption [21], biodegradation [22], ozone or Fenton oxidation technologies [23–25], and UV-based advanced oxidation processes [26,27]. However, none of these processes allows a complete ATZ removal [28].

Among the advanced oxidation technologies (AOPs) [29–34], heterogeneous photocatalysis represents one of most promising processes to decontaminate water from organic substances [35–45], such as ATZ [46–48]. Titanium dioxide (TiO_2) in nanometric form is the most used catalyst for water and wastewater photocatalytic treatments due to its low cost, high stability, and efficiency. The use of nanoparticles in photocatalysis is attractive because of their high surface/volume ratio and highly reactive surfaces which make them good sorbents of contaminants [49]. Nevertheless, the energy cost related to the UV light used for catalyst activation and the need to avoid the nano powders release into the effluent [49,50], remain the main constraints to full scale application. In order to make the process more sustainable by exploiting sunlight irradiation, TiO_2 can be doped with nitrogen, decreasing the band gap and increasing the absorption of visible light (Vis) [48,51–

53]. Likewise the nanopowders release into the effluents could be avoided by immobilising the photocatalyst inside suitable supports [54]. To date, the most used materials to immobilise the nanopowder photocatalysts are glass [54–56], ceramics [57–59] and polymers [60].

Polymeric materials proved to be very promising alternatives for developing green technologies and new devices [61–63]. Recent studies reported that composite materials based on thermoplastic polymers aerogels as supports for photocatalysts in powder form are economic, recyclable, and manageable systems [64–66]. The good mechanical properties and the nanoporous crystalline phase conferring high surface areas and good absorption properties make the monolithic aerogels of syndiotactic polystyrene (sPS) a promising support for catalytic applications [67].

Recent studies showed that monolithic composite aerogels sPS/N-doped TiO₂ (sPS/NdT) were more efficient than powder photocatalysts under both UV and visible (Vis) light to degrade methylene blue [66] and phenol [68].

Most scientific studies on photocatalytic degradation of biorecalcitrant pollutants focus on kinetics of the process and intermediates/by-products formation, leaving out ecotoxicological studies. To assess the possible environmental impact of the whole process, the absence of toxic effects of the process effluents should be evaluated [69]. It is also noteworthy that no paper reports toxicological results on the photocatalytic degradation of contaminants by using composite aerogels.

This research focused on photocatalytic degradation of ATZ by monolithic composite aerogel sPS/N-doped TiO₂ (sPS/NdT) under UV and Vis light. A battery of bioassays (i.e., *Aliivibrio fischeri*, *Raphidocelis subcapitata*, and *Daphnia magna*) was used to evaluate residual toxicity by a one-health perspective.

2. Materials and methods

2.1 Chemicals and reagents

Aerogels were prepared using a highly stereoregular syndiotactic polystyrene (sPS, syndiotactic triads over 98% determined by ^{13}C nuclear magnetic resonance) manufactured by Idemitsu Kosan Co., Ltd. (Japan), under the trademark XAREC[®] 90ZC.

Atrazine (CAS number: 1912-24-9, analytical standard, purity $\geq 98\%$) used to prepare the standard and sample solutions and titanium tetraisopropoxide (97 wt%) used to prepare N-doped TiO_2 photocatalysts were purchased from Sigma Aldrich (Germany).

Ammonia solution (30 wt%, analytic grade) used as nitrogen source for the preparation of NdT photocatalyst, chloroform (analytical grade) used for the preparation of high porosity composite aerogels, acetonitrile (HPLC gradient grade) and ultra-pure water (LC-MS grade) used for chromatographic analyses were purchased from Carlo Erba Reagents (France).

All solutions were prepared using ultrapurewater (Milli-Q[®] system Elix 10, Merck Millipore, Billarica, MA USA).

2.2 Composite photocatalyst preparation

N-doped TiO_2 (NdT) photocatalyst was prepared by the sol-gel method using ammonia as a nitrogen source and titanium tetraisopropoxide as described by Sacco et al. (2012). The obtained NdT sample is able to absorb visible light since its band gap energy is equal to 2.5 eV, as shown in our previous paper [70]

Monolithic composite aerogel sPS/NdT was prepared according to procedure reported by Sacco et al. (2018). In detail, syndiotactic polystyrene (sPS) polymer and NdT photocatalyst (90/10 weight ratio) were dispersed in chloroform, in hermetically sealed test tube, and heated at 100 °C. The suspension was subsequently cooled to room temperature forming a gel. The solvent was extracted from the gel by treating with supercritical carbon dioxide (ISCO SFX 220 extractor for 4 h at $T=40$ °C and $P= 20$ MPa) to obtain the relative monolithic composite aerogel. The amount of NdT photocatalyst dispersed in sPS used in this work was optimized in our previous paper in which SEM

analysis evidenced that NdT particles were uniformly dispersed within the fibrillary polymer network [68].

2.3 Composite photocatalyst characterization

To verify the correct preparation of the composite aerogel sPS/NdT, the crystalline structure of both the sPS polymer and NdT photocatalyst was analysed by using wide angle X-ray diffraction (WAXD). WAXD patterns were carried out using an automatic D8 Advance (Bruker, Billerica, MA USA) diffractometer in reflection geometry mode and with nickel filtered Cu-K α radiation. The intensities of WAXD patterns were not corrected for polarization and Lorentz factors, to allow easier comparison with most literature data. The 2θ acquisition interval range was between 5° and 80° , scanning with a step size of 0.0303° and an acquisition time of 0.200 s per point.

The specific surface area (SSA) of the aerogel was evaluated by static N₂ adsorption measurements at -196°C using a Nova 4200e analyser (Quantachrome Instruments, Boynton Beach, FL, USA), according to BET method.

The morphology of the sPS/NdT aerogel was characterized by means of a scanning electron microscope (SEM, Zeiss Evo50). Samples were prepared by fracturing small pieces of the aerogel. Before imaging, all the specimens were coated with gold using a VCR high resolution indirect ion-beam sputtering system. The samples were coated depositing approximately 20 nm of gold. The coating procedure was necessary in order to prevent surface charging during the measurement and to increase the image resolution.

2.4 Photocatalytic activity tests

Photocatalytic experiments were carried out in a previous optimized pyrex cylindrical photoreactor [71] (ID = 2.5 cm, h = 25 cm) equipped with an air distributor device ($Q_{\text{air}} = 150\text{ cm}^3/\text{min}$, at standard temperature and pressure), using 75 mL of ATZ aqueous solution (initial concentration

range 0.1–10 mg/L), a dosage of 0.4 g/L for the powder photocatalyst and 4 g/L for sPS/NdT (corresponding to 0.4 g/L of NdT dosage). Solutions were continuously mixed using an external recirculation system powered by a peristaltic pump (Watson Marlow 120s). UV-A (emission: 365 nm; irradiance 13 W/m²) or Vis (emission range: 400–800 nm; irradiance 16 W/m²) LEDs strips (NewOralight) were wrapped around the external surface of the pyrex tube for the irradiation of test solutions. Before each experiment, the system was kept in the dark for 60 min to reach the adsorption equilibrium of ATZ in the composite aerogel and then irradiated for 180 min.

ATZ concentrations were measured by high-performance liquid chromatography (HPLC) technique using an UltiMate 3000 system (Thermo Fisher Scientific, Waltham, MA USA), equipped with DAD detector, binary pump, column thermostat and automatic sample injector with 100 µL loop. The reversed-phase Luna 5u C18 column (150 mm × 4.6 mm i.d., pore size 5µm) (Phenomenex, Torrance, CA USA) was used for chromatographic separation at 25 °C. A mixture of acetonitrile/water (70/30 v/v) was used as mobile phase at an isocratic flow rate of 1.0 mL/min. The injection volume was 80 µL and the analysis were carried out at 221 nm that corresponds to maximum absorption of ATZ. The retention time of atrazine was to 2.95 ± 0.01 min. The limit of quantification was 0.010 mg/L that was the lowest concentration of the calibration curves (linear regression, R² > 0.99). The data were elaborated using the Dionex Chromeleon™ 6.8 software.

2.5 Bioassays and toxicity data analysis

Toxicity tests with the green alga *Raphidocelis subcapitata* were carried out according to the ISO 8692 (2012a).

Based on the results obtained for the pure substance (Table S1), a positive control (obtained by adding ISO algal medium to an aqueous solution containing 0.1 mg/L of atrazine) was regularly included in all tests with UV and Vis treated solutions. In the remainder of the present paper, we will refer to this positive control as ‘atrazine-spiked water’. Inhibition effects on algal growth after 72 h of exposure were assessed by cell counting using a BD Accuri C6 flow cytometer (see SI for

further details). Because of UV or Vis treatments can generate degradation products with potential toxic effects on organisms other than primary producers, selected UV and Vis treated solutions were also tested with the bacterium *A. fischeri* and the freshwater crustacean *D. magna* using the corresponding standardized procedures (ISO 11348-3, 1999; ISO 6341, 2012). Effects on bacterium and crustacean were assessed after 30 min and 24 h of exposure, respectively.

Replicate for toxicity test range from 2 to 6 (see SI). The median inhibition concentration (IC_{50}) (i.e., bacteria and microalgae) or effect concentration (EC_{50}) (i.e., crustaceans) (and the relative 95% confidence limit values) were estimated using the REGTOX Excel macro [72]. The percentage of effect adjusted to negative controls was provided for algae, bacteria, and daphnids exposed to effluents. Toxicity data were checked for normality (Shapiro-Wilk test) and homogeneity of variance (Bartlett's test). According to the results, parametric (one-way analysis of variance) or non-parametric (Kruskal-Wallis test) (i.e., if at least one test failed) methods were used to analyse data, also using a Tukey's *post-hoc* pairwise comparison.

For toxicity tests, the UV and Vis irradiation time in photocatalytic tests was prolonged up to 72 h.

2.6 Calculation of electric energy consumption

The electric energy consumption was evaluated for the UV and Vis photocatalytic processes using the $E_{E/O}$ value (UV and Vis light). The $E_{E/O}$ value, expressed in kWh in European countries, represents a scale-up parameter for removing 90% of a pollutant contained in 1 m³ of polluted water. $E_{E/O}$ values were estimated following Azbar et al. (2004) and Vaiano et al. (2019):

$$E_{E/O} = \frac{P \cdot t \cdot 1000}{V \cdot 60 \cdot \ln\left(\frac{C_0}{C_f}\right)} \quad (1)$$

where P is the nominal power of the light source (kW), t the irradiation time (minutes), V the volume solution (L), C_o the ATZ initial concentration (mg/L) and C_f the ATZ concentration after 72 h (mg/L).

3. Results and discussion

3.1 Aerogels characterization

The composite aerogel sPS/NdT WAXD pattern (Figure 1) showed the typical reflections of sPS crystalline nanoporous δ -phase in the 2θ range 8 - 23° (Figure 1, inset), as well as the reflections at 2θ higher than 23° of NdT powder in anatase phase [73]. This pattern proved the formation of the sPS/NdT composite.

Additionally, SSA of NdT and sPS was equal to 30 and 260 m²/g, respectively. On the other hand the SSA value of sPS/NdT was lower than sPS and equal to 222 m²/g, indicating that the presence of NdT powders in the sPS aerogel determined a decrease in specific surface area, which however remained higher than 200 m²/g because of the porous nature of the crystalline nanoporous δ -phase of sPS, in agreement with literature [66,74]

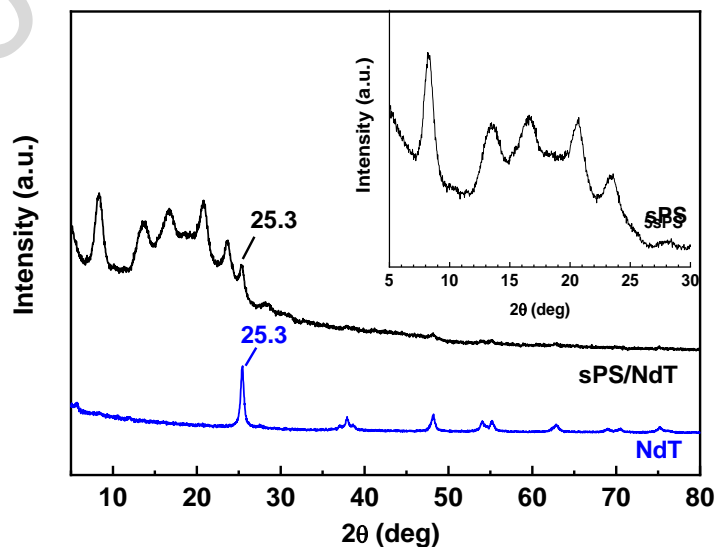


Figure 1. WAXD diffraction patterns: sPS/NdT aerogel (black line), NdT powder (blue line) and nanoporous δ -form of sPS (inset Figure 1).

3.2 Photocatalytic activity under UV and Vis light

3.2.1 Degradation tests

ATZ solutions at 0.1 mg/L were used for all the degradation experiments.

Preliminary photolysis experiments were carried out under UV and VIS light (Figure S1). For both irradiation conditions, a slightly decreased of ATZ concentration was observed only in the first 30 min of run time and then remained stable until the end of both tests. Such results evidenced the stability of ATZ molecules when the liquid medium is treated with only UV or VIS light and in the absence of photocatalyst.

Before to start photocatalytic process, a dark period of 60 min was established to reach a stationary equilibrium, for both NdT and sPS/NdT. An atrazine sorption of 6% and 14% for NdT catalyst and sPS/NdT, respectively could be observed after the dark phase (Figure 2). The ATZ removal by sPS/NdT and NdT, under UV and Vis irradiation, is reported in Figure 2a and 2b, respectively. Both processes clearly showed that after 180 min of irradiation time, the removal efficiency was higher for the sPS/NdT (47% and 25% under UV and Vis light irradiation, respectively) rather than the NdT (42% and 13% under UV and Vis light irradiation, respectively). Although sPS/NdT composite is always more active in the ATZ degradation than NdT powder, the degradation kinetics, faster for UV than Vis irradiation, were however very similar to each other. This result is very interesting since it is well known that, when a photocatalyst is immobilized in granular form or as thin film on macroscopic supports, the screening of the light by the support itself occurs and, moreover, the accessibility of the catalytic surface to the photons and to the reactants worsens,

inducing a photocatalytic activity significantly lower than that achieved when the photocatalysts are used in powder form [75–77].

On the contrary, in the case of sPS/NdT composite, the polymeric support allows to preserve the photocatalytic properties of NdT in powder form, minimizing the aggregation phenomena between photocatalyst particles, which typically occur in photocatalytic slurry reactors [68].

However, the overall greater removal efficiency demonstrated by sPS/NdT is essentially due to sPS aerogel contribution to ATZ sorption in the dark phase.

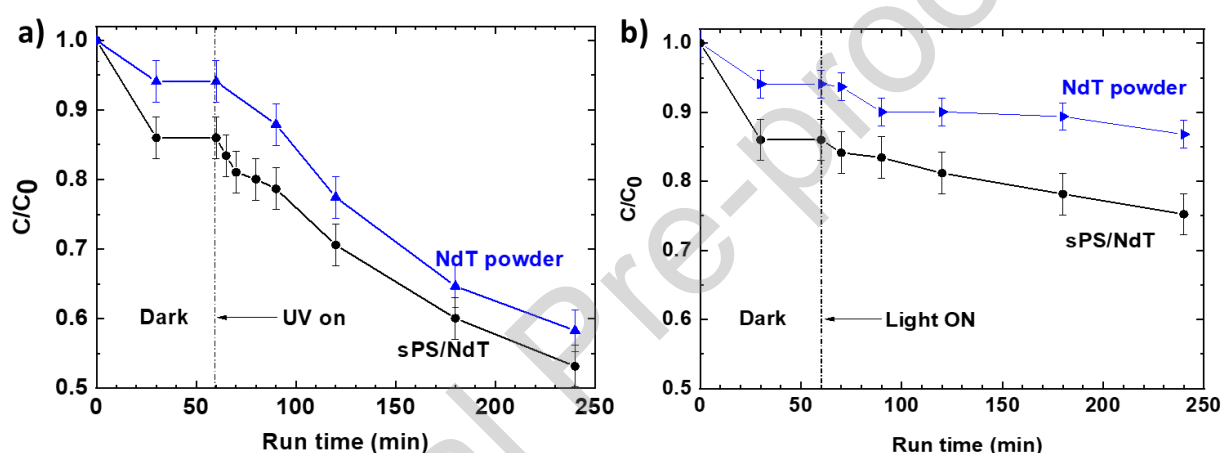


Figure 2. Atrazine removal by sPS/NdT composite aerogel and NdT powder: a) UV photocatalytic process; b) Visible photocatalytic process. Atrazine initial concentration: 0.1 mg/L. C and C_0 , concentration at $t = 0$ and t min, respectively.

3.2.2 Influence of atrazine initial concentration

The ATZ removal, by sPS/NdT under UV light irradiation, from solutions with different initial concentration (0.1, 1, and 10 mg/L), has been reported in Figure 3. An increase in contaminant concentration is expected to lead to a decrease in photocatalytic activity. When the number of pollutant molecules in solution increases, catalyst dosage begins to be inefficient for degradation of the contaminant since the number of reactive oxygen species generated during the irradiation is not enough to degrade the target pollutant [78]. In addition, the by-products or intermediates generated during the process could compete with atrazine molecules towards photocatalytic active sites,

resulting in a loss of efficiency [79]. Conversely, when sPS/NdT is used (Figure 3) the degradation performance was similar by increasing the atrazine initial concentration. The presence of aerogel polymeric matrix probably increases efficiency [66,68] and selectivity [64] of the process by discriminating between the different formed species, so as to allow the desorption of the possible intermediates generated under irradiation and avoid the deactivation of photoactive sites.

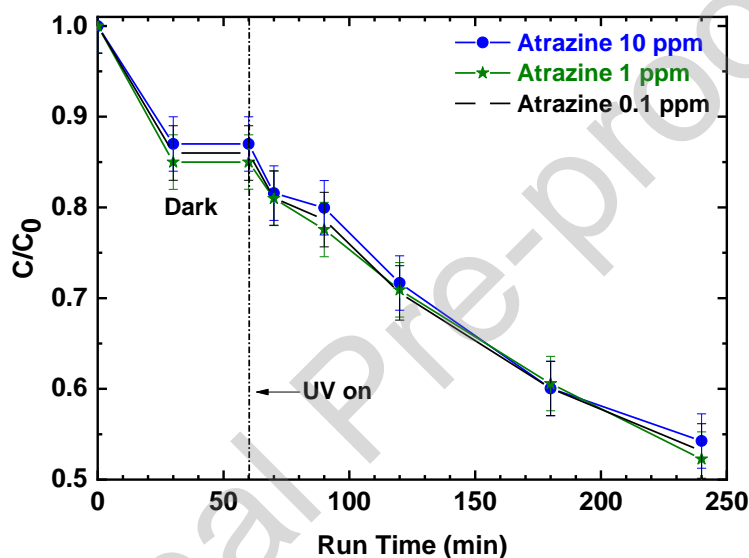


Figure 3. Atrazine removal by sPS/NdT at different initial atrazine concentration: 0.1 (black), 1 (green), and 10 (blue) mg/L.

3.2.2 Reusability evaluation

In order to assess the reusability of the composite aerogels, photocatalytic experiments were repeated five times under the same experimental conditions, using the same composite aerogel and fresh ATZ aqueous solutions under both UV and Vis irradiation (Figure 4).

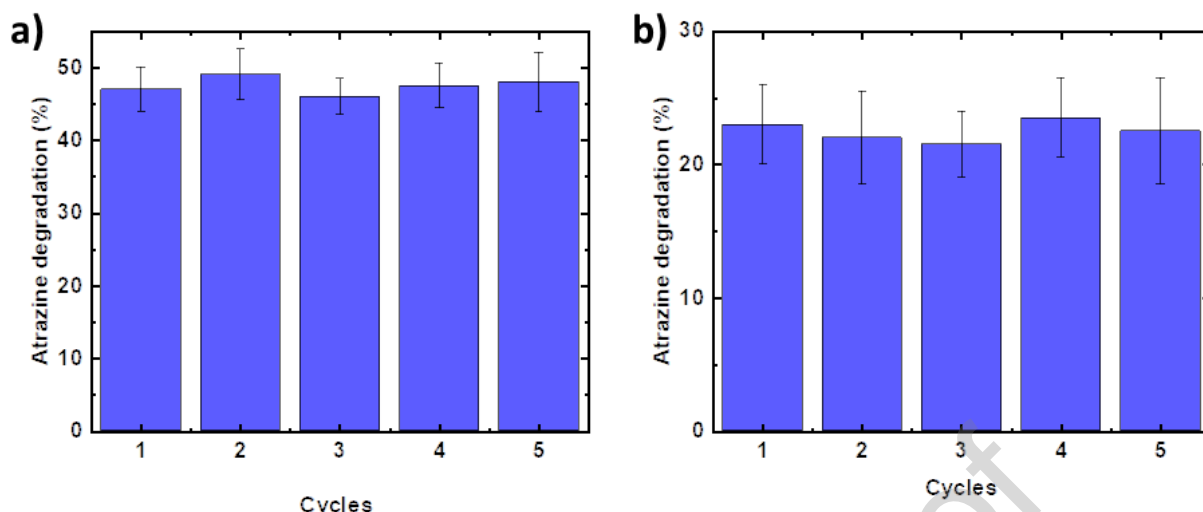


Figure 4. ATZ degradation (%) after 180 min of treatment for five cycles with the same sPS/NdT composite aerogel under: a) UV and b) Vis irradiation.

Results did not evidence any significant decrease of the photocatalytic activity according to previously published results obtained by using different photocatalysts dispersed on sPS matrix and used to remove methylene blue dye and phenol [66,68].

In addition, WAXD (Figure 5) and SEM analysis (Figure 6) were also carried out on the sPS/NdT aerogel before and after the reusability cycles (Figure 5).

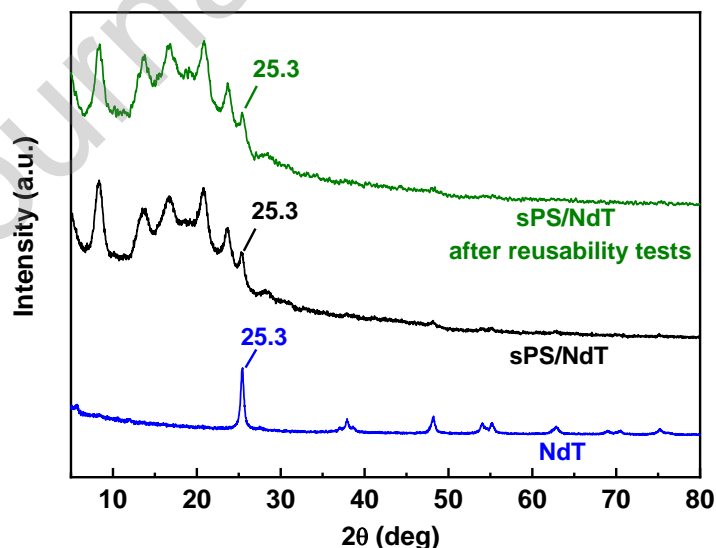


Figure 5. WAXD diffraction patterns: sPS/NdT aerogel (black line), NdT powder (blue line) and sPS/NdT aerogel after reusability tests (green line).

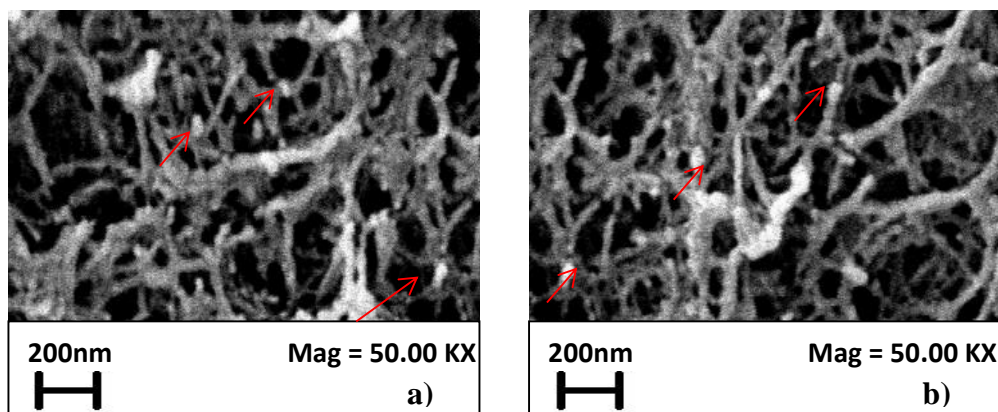


Figure 6. SEM images of a) sPS/NdT aerogel and b) sPS/NdT aerogel after reusability tests (some NdT particles dispersed in the aerogel are indicated by red arrows).

It can be seen from the WAXD spectra (Figure 5) that the NdT reflex (at $2\theta = 25.3^\circ$) of the sPS/NdT aerogel after the durability experiments remains unchanged. SEM images evidence that sPS/NdT (Figure 6a) exhibits an open network of fibrils with diameter of about 100 nm. Additionally, NdT particles (indicated by red arrows) appear uniformly dispersed within the fibrillary polymer network (white spots with main size of about 50 nm). From Figure 6b, it is possible to observe that the overall morphology of the aerogel did not change after the reusability tests and NdT particles within the polymer are still detectable. Thus, it is argued that the NdT particles are not released in the aqueous solution from the aerogel structure.

3.3 Toxicity results

The IC₅₀ of ATZ towards *R. subcapitata* was $39.6 \pm 6.3 \mu\text{g/L}$ ($n = 3$) similarly to Zhao et al. (2018) (i.e., $23 \mu\text{g/L}$, no confidence interval reported). The other two testing species, *A. fischeri* and *D. magna*, were less sensitive and did not allow the calculation of the EC₅₀s in the considered interval confirming previous literature data: i) EC₅₀ = 69.4 ($68.8\text{--}70.0$) mg/L [80] and EC₅₀ = 39.9 ($35.4\text{--}44.9$) mg/L [81] for *A. fischeri*; ii) EC₅₀ = 50.41 ± 2.64 mg/L for *D. magna* [82]. The toxicity of samples after UV and Vis sPS/NdT nanocomposite aerogels treatment was reported in Table 1.

Atrazine-spiked water after Vis treatment over 72 h (*i.e.*, ATZ residual concentration 70 $\mu\text{g/L}$) showed very high levels of toxicity towards microalgae with an almost total growth inhibition (99%) and a significant effect on the survival of *D. magna* (58% mortality after 24 h). Conversely, after UV treatment for 72 h (*i.e.*, atrazine residual concentration 18 $\mu\text{g/L}$) atrazine-spiked water appeared non-toxic to *D. magna* and had a very low effect on *R. subcapitata* growth and *A. fischeri* with an observed inhibition of 6.4%. UV treatment is highly more effective than Vis-one in removing ATZ and the related toxicity effects.

In Figure 7, the toxicity trend after 0.5, 1, 3, 24 and 72 h of Vis (Figure 7a) and UV (Figure 7b) treatments was summarized for all testing species including ATZ removal rates (*i.e.*, y-axis summarises both the percentage (%) of effect for toxicity testing and the removal rate (%) of ATZ). The trend of toxicity reduction/removal is apparent for all testing species, especially after 72 h of UV treatment even though ATZ was not completely removed (*i.e.*, up to approximately 80% removal rate). On the contrary, the Vis treatment was not effective in toxicity reduction, especially for *R. subcapitata*. The positive controls with 90 $\mu\text{g/L}$ of ATZ carried out during the experimental activity always showed a 70% inhibition effect (Table S2), confirming that the observed temporal trends reflected the actual changes in sample toxicity to *R. subcapitata*. The toxicity of samples to microalgae increased between 0.5 and 72 h for Vis treatment, and between 0.5 and 24 h for UV treatments, presuming that unidentified toxic by-products were formed as intermediates during both treatments. After 72 h of reaction time, UV photocatalysis successfully degraded the toxic by-products, eliminating most of the toxicity from the residual effluent. These observations confirm the need to systematically combine the development of advanced treatment processes with a toxicity evaluation of the treated water.

Table 1. ATZ treated samples (90% v/v) (whole sample exposure) considering both UV and Vis treatments after 72 h of irradiation. Data were expressed as percentage of effect (%) for all testing species.

Treatment	Values	<i>A. fischeri</i> (30 min)	<i>R. subcapitata</i> (72 h)	<i>D. magna</i> (24 h)
Vis	Mean	Non toxic	99.0%	58.3%
	Std.err.	-	0.2%	22.0%
UV	Mean	6.4%	6.4%	Non toxic
	Std.err.	1.6%	2.1%	-

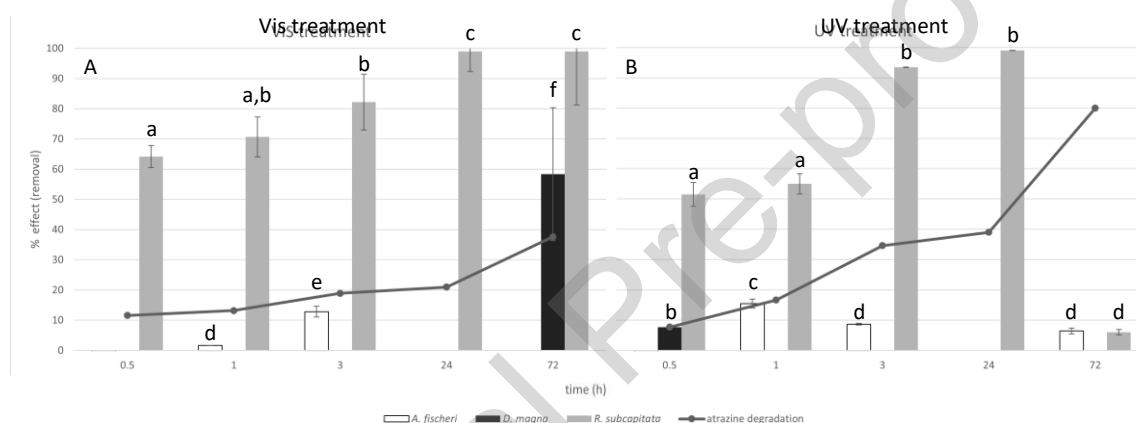


Figure 7. Effect of solutions initially amended with 100 µg/L of ATZ after visible (VIS) (A) and ultra-violet (UV) (B) treatment towards *A. fischeri*, *D. magna* and *R. subcapitata* following ATZ removal rate between 0.5-72 h. Data with different letters (a–f) are significantly different (Tukey's test, $p < 0.05$); y-axis reports both the percentage (%) of effect for toxicity testing and the removal rate (%) of ATZ.

The different toxicity behaviour observed under UV and VIS light could be explained considering the mechanism of ATZ photocatalytic degradation (Figure S2) reported in literature [52,83,84], in which hydroxyls are the main reactive oxygen species [85,86]. Two degradation pathways can occur during light irradiation: N-dealkylation and hydrolytic dechlorination. As also demonstrated by López-Muñoz et al. [84], the intermediates identified in the first steps of the degradation

pathways are dealkylated compounds, such as deethylatrazine (DEA) and deisopropylatrazine (DIA) (Figure S2). These compounds can show strong toxicity [87], therefore, they could be most likely responsible for the higher toxicity of solutions resulting from Vis photocatalytic process. In the case of UV treated solutions, where higher ATZ photocatalytic degradation performances were obtained after 72 h, the presence of cyanuric acid can be surmised. Previous research reports that, for long irradiation time, the s-triazine ring of ATZ remains intact and cyanuric acid is formed as the final stable product [88]. Cyanuric acid is known to be less toxic than ATZ and its other degradation products [89,90]. Such observations could explain the reduction in toxicity after 72 h of UV irradiation time.

The obtained results showed that, although it is desirable to develop a photocatalytic system capable of working in the presence of Vis light, it is necessary to evaluate, in the technological choice, the treatment times, the ability to remove toxicity but also the energy consumption required for the treatment. Despite the NdT catalyst can exploit the visible light leading to a progressive degradation of the target pollutant, the experimental data showed that, after 72 h of treatment time, the effluent appears still toxic. As a consequence, the calculus of electric energy consumption showed that the use of UV light ($E_{E/O} = 158 \text{ kWh/m}^3$) saves about 70 % of energy with respect to the use of Vis light ($E_{E/O} = 575 \text{ kWh/m}^3$).

Finally, the toxicity test results confirmed the need to systematically combine the study of advanced water treatment processes with a toxicity evaluation of the treated water, in order to correctly assess the environmental impact of the process itself.

4. Concluding remarks

A monolithic composite, based on N-doped TiO_2 (NdT) photocatalyst and syndiotactic polystyrene (sPS), was employed as a promising photocatalyst for the degradation of ATZ under UV and Vis

light irradiation. The photocatalytic results evidenced that sPS/NdT composite, in monolithic aerogel form, has better degradation performances than NdT catalyst in powder form, under both UV and Vis light irradiation, essentially because of sPS aerogel contribution to ATZ sorption in the dark phase. Moreover, the degradation performances of ATZ were similar by increasing the pollutant initial concentration when sPS/NdT was used, probably because the aerogel polymeric matrix is capable of discriminating between the species in solution, thus increasing the efficiency and selectivity of the catalytic process. Moreover, reusability studies showed any significant decrease of the photocatalytic activity after five treatment cycles. The toxicity test results indicated that, although a decrease of ATZ concentration was detected during the photocatalytic process under both UV and Vis irradiation, an increase in the solution toxicity, presumably due to more toxic by-products than ATZ itself, was observed. Only after 72 h of the UV irradiation, the solution appeared no toxic to *D. magna* and presented a very low effect to *R. subcapitata*. On the other hand, for Vis light tests, a very high level of toxicity was still detected even after 72 h of irradiation. These results confirmed that toxicity tests are an indispensable tool for a correct assessment of the environmental impact of the water treatment processes. Therefore, to make the photocatalytic technologies useful for a possible scale up technology it is essential to evaluate both the economical parameter in terms of ($E_{E/0}$) and the ecotoxicological data.

On the other hand, these results also indicate that sPS/NdT composite, in monolithic aerogel form, UV irradiated, has high removal efficiency of ATZ and its by-products. This composite catalytic system, which also exhibits high robustness and chemical stability and easy reusability after treatment, is promising for large-scale applications in advanced solar-based oxidation processes.

Acknowledgements

Wanda Navarra thanks to Erasmus⁺ Programme: mobility for traineeship 2018/2019-2019/2020.

Wanda Navarra was supported by a grant from PON “Ricerca e Innovazione 2014-2020” – Dottorati Innovativi con caratterizzazione industriale. The financial support of POR FESR CAMPANIA 2014/2020 - O.S. 1.1, is also gratefully acknowledged.

The financial support of University of Salerno through FARB2018 (ORSA185812) grant awarded to prof. Maurizio Carotenuto is also acknowledged.

References

- [1] R.P. Singh, N. Banerjee, Exploring the Influence of Celebrity Credibility on Brand Attitude, Advertisement Attitude and Purchase Intention, *Global Business Review*. 19 (2018) 1622–1639. <https://doi.org/10.1177/0972150918794974>.
- [2] Atrazine Market by Type, Size, Share and Global Forecast - 2027 | MRFR, (n.d.). <https://www.marketresearchfuture.com/reports/atrazine-market-7128> (accessed July 29, 2021).
- [3] E. Nelkenbaum, I. Dror, B. Berkowitz, Reductive dechlorination of atrazine catalyzed by metalloporphyrins, *Chemosphere*. 75 (2009) 48–55. <https://doi.org/10.1016/j.chemosphere.2008.11.074>.
- [4] T. Cavas, In vivo genotoxicity evaluation of atrazine and atrazine-based herbicide on fish *Carassius auratus* using the micronucleus test and the comet assay, *Food and Chemical Toxicology*. 49 (2011) 1431–1435. <https://doi.org/10.1016/j.fct.2011.03.038>.
- [5] M. Bisson, A. Hontela, Cytotoxic and Endocrine-Disrupting Potential of Atrazine, Diazinon, Endosulfan, and Mancozeb in Adrenocortical Steroidogenic Cells of Rainbow Trout Exposed in Vitro, *Toxicology and Applied Pharmacology*. 180 (2002) 110–117. <https://doi.org/10.1006/taap.2002.9377>.
- [6] M.K. Morgan, TERATOGENIC POTENTIAL OF ATRAZINE AND 2,4-D USING FETAX, *Null*. 48 (1996) 151–168. <https://doi.org/10.1080/009841096161401>.
- [7] Freeman Laura E. Beane, Rusiecki Jennifer A., Hoppin Jane A., Lubin Jay H., Koutros Stella, Andreotti Gabriella, Zahm Shelia Hoar, Hines Cynthia J., Coble Joseph B., Barone-Adesi Francesco, Sloan Jennifer, Sandler Dale P., Blair Aaron, Alavanja Michael C.R., Atrazine and Cancer Incidence Among Pesticide Applicators in the Agricultural Health Study (1994–2007), *Environmental Health Perspectives*. 119 (2011) 1253–1259. <https://doi.org/10.1289/ehp.1103561>.
- [8] G.P. Hayes, Rapid source characterization of the 2011 Mw 9.0 off the Pacific coast of Tohoku Earthquake, *Earth, Planets and Space*. 63 (2011) 4. <https://doi.org/10.5047/eps.2011.05.012>.
- [9] N.E. Omran, W.M. Salama, The endocrine disruptor effect of the herbicides atrazine and glyphosate on *Biomphalaria alexandrina* snails, *Toxicol Ind Health*. 32 (2016) 656–665. <https://doi.org/10.1177/0748233713506959>.
- [10] A.L.F. Destro, S.B. Silva, K.P. Gregório, J.M. de Oliveira, A.A. Lozi, J.A.S. Zuanon, A.L. Salaro, S.L.P. da Matta, R.V. Gonçalves, M.B. Freitas, Effects of subchronic exposure to environmentally relevant concentrations of the herbicide atrazine in the Neotropical fish *Astyanax altiparanae*, *Ecotoxicology and Environmental Safety*. 208 (2021) 111601. <https://doi.org/10.1016/j.ecoenv.2020.111601>.
- [11] EUR-Lex - 32013L0039 - EN - EUR-Lex, (n.d.). <https://eur-lex.europa.eu/legal-content/EN/ALL/?uri=celex%3A32013L0039> (accessed February 2, 2021).
- [12] EUR-Lex - 32008L0105 - EN - EUR-Lex, (n.d.). <https://eur-lex.europa.eu/legal-content/EN/ALL/?uri=celex%3A32008L0105> (accessed February 2, 2021).

- [13] N. Udiković-Kolić, C. Scott, F. Martin-Laurent, Evolution of atrazine-degrading capabilities in the environment, *Appl Microbiol Biotechnol.* 96 (2012) 1175–1189. <https://doi.org/10.1007/s00253-012-4495-0>.
- [14] J. Mahía, A. Martín, T. Carballas, Atrazine degradation and enzyme activities in an agricultural soil under two tillage systems, *The Science of the Total Environment.* 378 (2007) 187–94. <https://doi.org/10.1016/j.scitotenv.2007.01.036>.
- [15] P. Ghosh, L. Philip, Environmental significance of atrazine in aqueous systems and its removal by biological processes: An overview, *Global NEST J.* 8 (2006).
- [16] J. Sun, L. Pan, Y. Zhan, D. Tsang, L. Zhu, X.-D. Li, Atrazine contamination in agricultural soils from the Yangtze River Delta of China and associated health risks, *Environmental Geochemistry and Health.* 39 (2017). <https://doi.org/10.1007/s10653-016-9853-x>.
- [17] M.J.M. Bueno, M. Gomez, S. Herrera, M. Hernando, A. Agüera, A. Fernández-Alba, Occurrence and persistence of organic emerging contaminants and priority pollutants in five sewage treatment plants of Spain: two years pilot survey monitoring, *Environ Pollut.* 164 (2012) 267–273. <https://doi.org/10.1016/j.envpol.2012.01.038>.
- [18] J. Campo, A. Masiá, C. Blasco, Y. Picó, Occurrence and removal efficiency of pesticides in sewage treatment plants of four Mediterranean River Basins, *J Hazard Mater.* 263 Pt 1 (2013) 146–157. <https://doi.org/10.1016/j.jhazmat.2013.09.061>.
- [19] M.J. Benotti, R.A. Trenholm, B.J. Vanderford, J.C. Holady, B.D. Stanford, S.A. Snyder, Pharmaceuticals and Endocrine Disrupting Compounds in U.S. Drinking Water, *Environ. Sci. Technol.* 43 (2009) 597–603. <https://doi.org/10.1021/es801845a>.
- [20] M. Kamaz, S. Jones, X. Qian, M. Watts, W. Zhang, R. Wickramasinghe, Atrazine Removal from Municipal Wastewater Using a Membrane Bioreactor, *International Journal of Environmental Research and Public Health.* 17 (2020) 2567. <https://doi.org/10.3390/ijerph17072567>.
- [21] Z. Moeini, A. Azhdarpoor, S. Yousefinejad, H. Hashemi, Removal of atrazine from water using titanium dioxide encapsulated in salicylaldehydeNH₂MIL-101 (Cr): Adsorption or oxidation mechanism, *Journal of Cleaner Production.* 224 (2019) 238–245. <https://doi.org/10.1016/j.jclepro.2019.03.236>.
- [22] L. Wackett, M. Sadowsky, B. Martinez, N. Shapir, Biodegradation of atrazine and related s-triazine compounds: from enzymes to field studies, *Applied Microbiology and Biotechnology.* 58 (2002) 39–45. <https://doi.org/10.1007/s00253-001-0862-y>.
- [23] J.L. Acero, K. Stemmler, U. von Gunten, Degradation Kinetics of Atrazine and Its Degradation Products with Ozone and OH Radicals: A Predictive Tool for Drinking Water Treatment, *Environ. Sci. Technol.* 34 (2000) 591–597. <https://doi.org/10.1021/es990724e>.
- [24] S. Nélieu, L. Kerhoas, J. Einhorn, Degradation of Atrazine into Ammeline by Combined Ozone/Hydrogen Peroxide Treatment in Water, *Environ. Sci. Technol.* 34 (2000) 430–437. <https://doi.org/10.1021/es980540k>.
- [25] R. VENKATADRI, R.W. PETERS, Chemical Oxidation Technologies: Ultraviolet Light/Hydrogen Peroxide, Fenton's Reagent, and Titanium Dioxide-Assisted Photocatalysis, *Hazardous Waste and Hazardous Materials.* 10 (1993) 107–149. <https://doi.org/10.1089/hwm.1993.10.107>.
- [26] F.J. Beltrán, G. Ovejero, B. Acedo, Oxidation of atrazine in water by ultraviolet radiation combined with hydrogen peroxide, *Water Research.* 27 (1993) 1013–1021. [https://doi.org/10.1016/0043-1354\(93\)90065-P](https://doi.org/10.1016/0043-1354(93)90065-P).
- [27] A. De Luca, R.F. Dantas, A.S.M. Simões, I.A.S. Toscano, G. Lofrano, A. Cruz, S. Esplugas, Atrazine Removal in Municipal Secondary Effluents by Fenton and Photo-Fenton Treatments, *Chemical Engineering & Technology.* 36 (2013) 2155–2162. <https://doi.org/10.1002/ceat.201300135>.
- [28] A. Giwa, A. Yusuf, H.A. Balogun, N.S. Sambudi, M.R. Bilad, I. Adeyemi, S. Chakraborty, S. Curcio, Recent advances in advanced oxidation processes for removal of contaminants from water: A comprehensive review, *Process Safety and Environmental Protection.* 146 (2021) 220–256. <https://doi.org/10.1016/j.psep.2020.08.015>.

- [29] M. Ahmadian, M. Pirsaeheb, H. Janjani, H. Hossaini, Ultraviolet activated persulfate based AOP for MTBE decomposition in aqueous solution, *Desalination and Water Treatment*. 161 (2019) 269–274. <https://doi.org/10.5004/dwt.2019.24310>.
- [30] M. Pirsaeheb, H. Hossaini, N.K. Raad, S. Kianpour, H. Hossini, A systematic review on photo-Fenton process as an efficient advanced oxidation for degradation of amoxicillin in aqueous environments, *Reviews on Environmental Health*. (2022). <https://doi.org/10.1515/reveh-2021-0155>.
- [31] F. Asgharzadeh, M. Moradi, A. Jonidi jafari, A. Esrafil, M. Tahergorabi, R. Rezaei Kalantary, Enhanced electro kinetic- pseudo-Fenton degradation of pyrene - contaminated soil using Fe₃O₄ magnetic nanoparticles: A data set, *Data in Brief*. 24 (2018). <https://doi.org/10.1016/j.dib.2018.11.068>.
- [32] M. Pirsaeheb, H. Hossaini, J. Amini, Evaluation of a zeolite/anaerobic baffled reactor hybrid system for treatment of low bio-degradable effluents, *Materials Science and Engineering: C*. 104 (2019) 109943. <https://doi.org/10.1016/j.msec.2019.109943>.
- [33] M. Pirsaeheb, H. Sorkali, N. Fattahi, N. Noori, preconcentration and determination of amoxicillin and ceftriaxone in hospital sewage using vortex-assisted liquid-phase microextraction based on the solidification of the deep eutectic solvent followed by HPLC–UV, *International Journal of Environmental Analytical Chemistry*. 99 (2019) 1–12. <https://doi.org/10.1080/03067319.2019.1576866>.
- [34] M. Pirsaeheb, H. Hossaini, H. Janjani, An overview on ultraviolet persulfate based advanced oxidation process for removal of antibiotics from aqueous solutions: a systematic review, *DESALINATION AND WATER TREATMENT*. 165 (2019) 382–395. <https://doi.org/10.5004/dwt.2019.24559>.
- [35] M. Irandost, R. Akbarzadeh, M. Pirsaeheb, A. Asadi, P. Mohammadi, M. Sillanpää, Fabrication of highly visible active N, S co-doped TiO₂@MoS₂ heterojunction with synergistic effect for photocatalytic degradation of diclofenac: Mechanisms, modeling and degradation pathway, *Journal of Molecular Liquids*. (2019).
- [36] N. Farhadian, R. Akbarzadeh, M. Pirsaeheb, T.-C. Jen, Y. Fakhri, A. Asadi, Chitosan modified N, S-doped TiO₂ and N, S-doped ZnO for visible light photocatalytic degradation of tetracycline, *International Journal of Biological Macromolecules*. 132 (2019) 360–373. <https://doi.org/10.1016/j.ijbiomac.2019.03.217>.
- [37] R.R. Kalantary, M. Moradi, M. Pirsaeheb, A. Esrafil, A.J. Jafari, M. Gholami, Y. Vasseghian, E. Antolini, E.-N. Dragoi, Enhanced photocatalytic inactivation of *E. coli* by natural pyrite in presence of citrate and EDTA as effective chelating agents: Experimental evaluation and kinetic and ANN models, *Journal of Environmental Chemical Engineering*. 7 (2019) 102906. <https://doi.org/10.1016/j.jece.2019.102906>.
- [38] M. Pirsaeheb, K. Karimi, B. Shahmoradi, M. Moradi, Y. Vasseghian, E. Dragoi, Photocatalyzed degradation of acid orange 7 dye under sunlight and ultraviolet irradiation using Ni- doped ZnO nanoparticles, *Desalination and Water Treatment*. 165 (2019) 321–332. <https://doi.org/10.5004/dwt.2019.24462>.
- [39] M. Moradi, R.R. Kalantary, A. Esrafil, A.J. Jafari, M. Gholami, Visible light photocatalytic inactivation of *Escherichia coli* by natural pyrite assisted by oxalate at neutral pH, *Journal of Molecular Liquids*. 248 (2017) 880–889. <https://doi.org/10.1016/j.molliq.2017.10.115>.
- [40] M. Pirsaeheb, B. Shahmoradi, M. Beikmohammadi, E. Azizi, H. Hossini, G. Md Ashraf, Photocatalytic degradation of Aniline from aqueous solutions under sunlight illumination using immobilized Cr:ZnO nanoparticles, *Scientific Reports*. 7 (2017) 1473. <https://doi.org/10.1038/s41598-017-01461-5>.
- [41] H. Arfaeina, H. Sharafi, M. Moradi, M. Ehsanifar, S. Hashemi, Efficient degradation of 4-chloro-2-nitrophenol using photocatalytic ozonation with nano-zinc oxide impregnated granular activated carbon (ZNO–GAC), *DESALINATION AND WATER TREATMENT*. 93 (2017) 145–151. <https://doi.org/10.5004/dwt.2017.21427>.
- [42] B. Shahmoradi, M. Pirsaeheb, M.A. Pordel, T. Khosravi, Dr.R. Pawar, S. Lee, Photocatalytic performance of chromium-doped TiO₂ nanoparticles for degradation of Reactive Black 5 under natural sunlight illumination, *DESALINATION AND WATER TREATMENT*. 67 (2017) 324–331. <https://doi.org/10.5004/dwt.2017.20373>.

- [43] B. Shahmoradi, M.A. Pordel, M. Pirsaeheb, A. Maleki, S. Kohzadi, Y. Gong, R.R. Pawar, S.-M. Lee, H.P. Shivaraju, G. McKay, Synthesis and characterization of barium-doped TiO₂ nanocrystals for photocatalytic degradation of Acid Red 18 under solar irradiation, (n.d.) 1.
- [44] M. Pirsaeheb, B. Shahmoradi, T. Khosravi, K. Karimi, Y. Zandsalimi, Solar degradation of malachite green using nickel-doped TiO₂ nanocatalysts, *Null.* 57 (2016) 9881–9888. <https://doi.org/10.1080/19443994.2015.1033764>.
- [45] D.J. Naghan, A. Azari, N. Mirzaei, A. Velayati, F.A. Tapouk, S. Adabi, M. Pirsaeheb, K. Sharafi, Parameters effecting on photocatalytic degradation of the phenol from aqueous solutions in the presence of ZnO nanocatalyst under irradiation of UV-C light, (n.d.) 5.
- [46] M.R. Hoffmann, S.T. Martin, W. Choi, D.W. Bahnemann, Environmental Applications of Semiconductor Photocatalysis, *Chem. Rev.* 95 (1995) 69–96. <https://doi.org/10.1021/cr00033a004>.
- [47] A. Mills, S. Le Hunte, An overview of semiconductor photocatalysis, *Journal of Photochemistry and Photobiology A: Chemistry.* 108 (1997) 1–35. [https://doi.org/10.1016/S1010-6030\(97\)00118-4](https://doi.org/10.1016/S1010-6030(97)00118-4).
- [48] O. Sacco, V. Vaiano, C. Han, D. Sannino, D.D. Dionysiou, Photocatalytic removal of atrazine using N-doped TiO₂ supported on phosphors, *Applied Catalysis B: Environmental.* 164 (2015) 462–474. <https://doi.org/10.1016/j.apcatb.2014.09.062>.
- [49] V. Nogueira, I. Lopes, T.A.P. Rocha-Santos, M.G. Rasteiro, N. Abrantes, F. Gonçalves, A.M.V.M. Soares, A.C. Duarte, R. Pereira, Assessing the ecotoxicity of metal nano-oxides with potential for wastewater treatment, *Environmental Science and Pollution Research.* 22 (2015) 13212–13224. <https://doi.org/10.1007/s11356-015-4581-9>.
- [50] D. Minetto, G. Libralato, A. Volpi Ghirardini, Ecotoxicity of engineered TiO₂ nanoparticles to saltwater organisms: An overview, *Environment International.* 66 (2014) 18–27. <https://doi.org/10.1016/j.envint.2014.01.012>.
- [51] I.K. Konstantinou, T.M. Sakellarides, V.A. Sakkas, T.A. Albanis, Photocatalytic Degradation of Selected s-Triazine Herbicides and Organophosphorus Insecticides over Aqueous TiO₂ Suspensions, *Environ. Sci. Technol.* 35 (2001) 398–405. <https://doi.org/10.1021/es001271c>.
- [52] E. Pelizzetti, V. Maurino, C. Minero, V. Carlin, M.L. Tosato, E. Pramauro, O. Zerbini, Photocatalytic degradation of atrazine and other s-triazine herbicides, *Environ. Sci. Technol.* 24 (1990) 1559–1565. <https://doi.org/10.1021/es00080a016>.
- [53] I. Texier, J. Ouazzani, J. Delaire, C. Giannotti, Study of the mechanisms of the photodegradation of atrazine in the presence of two photocatalysts: TiO₂ and Na₄W₁₀O₃₂, *Tetrahedron.* 55 (1999) 3401–3412. [https://doi.org/10.1016/S0040-4020\(98\)01150-8](https://doi.org/10.1016/S0040-4020(98)01150-8).
- [54] T.A. McMurray, P. Dunlop, J. Byrne, The photocatalytic degradation of atrazine on nanoparticulate TiO₂ films, *Journal of Photochemistry and Photobiology A: Chemistry.* 182 (2006) 43–51. <https://doi.org/10.1016/j.jphotochem.2006.01.010>.
- [55] Balasubramanian G, Dionysiou DD, Suidan MT, Baudin I, Audin B, Laine JM, Evaluating the activities of immobilized TiO₂ powder films for the photocatalytic degradation of organic contaminants in water, *Appl. Catal. B: Environ.* 47 (2004) 73–84. <https://doi.org/10.1016/j.apcatb.2003.04.002>.
- [56] M. Karches, M. Morstein, P. Rudolf von Rohr, R. Pozzo, J. Giombi, M. Baltanas, Plasma-CVD-coated glass beads as photocatalyst for water decontamination, *Catalysis Today.* 72 (2002) 267–279. [https://doi.org/10.1016/S0920-5861\(01\)00505-3](https://doi.org/10.1016/S0920-5861(01)00505-3).
- [57] T.L.R. Hewer, S. Suárez, J.M. Coronado, R. Portela, P. Avila, B. Sanchez, Hybrid photocatalysts for the degradation of trichloroethylene in air, *Catalysis Today.* 143 (2009) 302–308. <https://doi.org/10.1016/j.cattod.2009.02.001>.
- [58] S. Suárez, J.M. Coronado, R. Portela, J.C. Martín, M. Yates, P. Avila, B. Sánchez, On the Preparation of TiO₂–Sepiolite Hybrid Materials for the Photocatalytic Degradation of TCE: Influence of TiO₂ Distribution in the Mineralization, *Environ. Sci. Technol.* 42 (2008) 5892–5896. <https://doi.org/10.1021/es703257w>.
- [59] A.H. Cheshme Khavar, G. Moussavi, A.R. Mahjoub, M. Satari, Facile preparation of multi-doped TiO₂/rGO cross-linked 3D aerogel (GaNF@TGA) nanocomposite as an efficient visible-light activated

- catalyst for photocatalytic oxidation and detoxification of atrazine, *Solar Energy*. 173 (2018) 848–860. <https://doi.org/10.1016/j.solener.2018.08.034>.
- [60] T. Kemmitt, N.I. Al-Salim, M. Waterland, V.J. Kennedy, A. Markwitz, Photocatalytic titania coatings, *Current Applied Physics*. 4 (2004) 189–192. <https://doi.org/10.1016/j.cap.2003.11.006>.
- [61] A. Botta, S. Pragliola, V. Vincenzo, A. Rubino, S. Aprano, A. De Girolamo Del Mauro, M. Maglione, C. Minarini, Highly isotactic poly(N-pentenyl-carbazole): A challenging polymer for optoelectronic applications, *AIP Conference Proceedings*. 1599 (2014) 493–497. <https://doi.org/10.1063/1.4876886>.
- [62] A. Botta, C. Costabile, V. Venditto, S. Pragliola, R. Liguori, A. Rubino, D. Alberga, M. Savarese, C. Adamo, Optoelectronic properties of poly(N-alkenyl-carbazole)s driven by polymer stereoregularity, *Journal of Polymer Science Part A: Polymer Chemistry*. 56 (2018) 242–251. <https://doi.org/10.1002/pola.28899>.
- [63] S. Pragliola, R. Vita, P. Longo, Aqueous emulsion polymerization of styrene and substituted styrenes using titanocene compounds, *Polymer*. 54 (2013) 1583–1587. <https://doi.org/10.1016/j.polymer.2013.01.017>.
- [64] O. Sacco, V. Vaiano, C. Daniel, W. Navarra, V. Venditto, Highly Robust and Selective System for Water Pollutants Removal: How to Transform a Traditional Photocatalyst into a Highly Robust and Selective System for Water Pollutants Removal, *Nanomaterials (Basel)*. 9 (2019). <https://doi.org/10.3390/nano9111509>.
- [65] S. Singh, H. Mahalingam, P.K. Singh, Polymer-supported titanium dioxide photocatalysts for environmental remediation: A review, *Applied Catalysis A: General*. 462–463 (2013) 178–195. <https://doi.org/10.1016/j.apcata.2013.04.039>.
- [66] V. Vaiano, O. Sacco, D. Sannino, P. Ciambelli, S. Longo, V. Venditto, G. Guerra, N-doped TiO₂/s-PS aerogels for photocatalytic degradation of organic dyes in wastewater under visible light irradiation, *Journal of Chemical Technology & Biotechnology*. 89 (2014) 1175–1181. <https://doi.org/10.1002/jctb.4372>.
- [67] C. Daniel, S. Longo, R. Ricciardi, E. Reverchon, G. Guerra, Monolithic Nanoporous Crystalline Aerogels, *Macromolecular Rapid Communications*. 34 (2013) 1194–1207. <https://doi.org/10.1002/marc.201300260>.
- [68] O. Sacco, V. Vaiano, C. Daniel, W. Navarra, V. Venditto, Removal of phenol in aqueous media by N-doped TiO₂ based photocatalytic aerogels, *Materials Science in Semiconductor Processing*. 80 (2018) 104–110. <https://doi.org/10.1016/j.mssp.2018.02.032>.
- [69] G. Libralato, G. Lofrano, A. Siciliano, E. Gambino, G. Boccia, C. Federica, A. Francesco, E. Galdiero, R. Gesuele, M. Guida, 8 - Toxicity assessment of wastewater after advanced oxidation processes for emerging contaminants' degradation*, in: O. Sacco, V. Vaiano (Eds.), *Visible Light Active Structured Photocatalysts for the Removal of Emerging Contaminants*, Elsevier, 2020: pp. 195–211. <https://doi.org/10.1016/B978-0-12-818334-2.00008-0>.
- [70] O. Sacco, M. Stoller, V. Vaiano, P. Ciambelli, A. Chianese, D. Sannino, Photocatalytic Degradation of Organic Dyes under Visible Light on N-Doped TiO₂ Photocatalysts, *International Journal of Photoenergy*. 2012 (2012). <https://doi.org/10.1155/2012/626759>.
- [71] V. Vaiano, O. Sacco, M. Stoller, A. Chianese, P. Ciambelli, D. Sannino, Influence of the Photoreactor Configuration and of Different Light Sources in the Photocatalytic Treatment of Highly Polluted Wastewater, *International Journal of Chemical Reactor Engineering*. 12 (2014) 63–75. <https://doi.org/10.1515/ijcre-2013-0090>.
- [72] https://www.normalesup.org/~vindimian/en_download.html, (n.d.). https://www.normalesup.org/~vindimian/en_download.html (accessed July 29, 2021).
- [73] O. Sacco, M. Stoller, V. Vaiano, P. Ciambelli, A. Chianese, D. Sannino, Photocatalytic Degradation of Organic Dyes under Visible Light on N-Doped Photocatalysts, *International Journal of Photoenergy*. 2012 (2012) e626759. <https://doi.org/10.1155/2012/626759>.
- [74] C. Daniel, S. Giudice, G. Guerra, Syndiotactic Polystyrene Aerogels with β , γ , and ϵ Crystalline Phases, *Chem. Mater.* 21 (2009) 1028–1034. <https://doi.org/10.1021/cm802537g>.

- [75] M.F.J. Dijkstra, H. Buwalda, A.W.F. de Jong, A. Michorius, J.G.M. Winkelman, A.A.C.M. Beenackers, Experimental comparison of three reactor designs for photocatalytic water purification, *Chemical Engineering Science*. 56 (2001) 547–555. [https://doi.org/10.1016/S0009-2509\(00\)00259-1](https://doi.org/10.1016/S0009-2509(00)00259-1).
- [76] A.S. El-Kalliny, S.F. Ahmed, L.C. Rietveld, P.W. Appel, Immobilized photocatalyst on stainless steel woven meshes assuring efficient light distribution in a solar reactor, *Drinking Water Engineering and Science*. 7 (2014) 41–52. <https://doi.org/10.5194/dwes-7-41-2014>.
- [77] A.J. Feitz, B.H. Boyden, T.D. Waite, Evaluation of two solar pilot scale fixed-bed photocatalytic reactors, *Water Research*. 34 (2000) 3927–3932. [https://doi.org/10.1016/S0043-1354\(00\)00153-6](https://doi.org/10.1016/S0043-1354(00)00153-6).
- [78] H.S. Wahab, A.A. Hussain, Photocatalytic oxidation of phenol red onto nanocrystalline TiO₂ particles, *J Nanostruct Chem*. 6 (2016) 261–274. <https://doi.org/10.1007/s40097-016-0199-9>.
- [79] J.M. Dangwang Dikdim, Y. Gong, G.B. Noumi, J.M. Sieliechi, X. Zhao, N. Ma, M. Yang, J.B. Tchatchueng, Peroxymonosulfate improved photocatalytic degradation of atrazine by activated carbon/graphitic carbon nitride composite under visible light irradiation, *Chemosphere*. 217 (2019) 833–842. <https://doi.org/10.1016/j.chemosphere.2018.10.177>.
- [80] P. Palma, V. Palma, R. Fernandes, A.M.V.M. Soares, I. Barbosa, Acute toxicity of atrazine, endosulfan sulphate and chlorpyrifos to *Vibrio fischeri*, *Thamnocephalus platyurus* and *Daphnia magna*, relative to their concentrations in surface waters from the Alentejo region of Portugal, *Bull Environ Contam Toxicol*. 81 (2008) 485–489. <https://doi.org/10.1007/s00128-008-9517-3>.
- [81] P.B. Tchounwou, B. Wilson, A. Ishaque, R. Ransome, M.-J. Huang, J. Leszczynski, Toxicity Assessment of Atrazine and Related Triazine Compounds in the Microtox Assay, and Computational Modeling for Their Structure-Activity Relationship, *International Journal of Molecular Sciences*. 1 (2000) 63–74. <https://doi.org/10.3390/ijms1040063>.
- [82] R.A. Moreira, A. da S. Mansano, L.C. da Silva, O. Rocha, A comparative study of the acute toxicity of the herbicide atrazine to cladocerans *Daphnia magna*, *Ceriodaphnia silvestrii* and *Macrothrix flabelligera*, *Acta Limnologica Brasiliensia*. (2014). <https://www.biodiversitylibrary.org/part/139347>.
- [83] G. Granados-Oliveros, E.A. Páez-Mozo, F.M. Ortega, C. Ferronato, J.-M. Chovelon, Degradation of atrazine using metalloporphyrins supported on TiO₂ under visible light irradiation, *Applied Catalysis B: Environmental*. 89 (2009) 448–454. <https://doi.org/10.1016/j.apcatb.2009.01.001>.
- [84] M.J. López-Muñoz, J. Aguado, A. Revilla, Photocatalytic removal of s-triazines: Evaluation of operational parameters, *Catalysis Today*. 161 (2011) 153–162. <https://doi.org/10.1016/j.cattod.2010.10.076>.
- [85] S. Sun, H. He, C. Yang, Y. Cheng, Y. Liu, Effects of Ca²⁺ and fulvic acids on atrazine degradation by nano-TiO₂: Performances and mechanisms, *Scientific Reports*. 9 (2019) 8880. <https://doi.org/10.1038/s41598-019-45086-2>.
- [86] W. Navarra, I. Ritacco, O. Sacco, L. Caporaso, M. Farnesi Camellone, V. Venditto, V. Vaiano, Density Functional Theory Study and Photocatalytic Activity of ZnO/N-Doped TiO₂ Heterojunctions, *J. Phys. Chem. C*. 126 (2022) 7000–7011. <https://doi.org/10.1021/acs.jpcc.2c00152>.
- [87] M. New-Aaron, Z. Naveed, E.G. Rogan, Estrogen Disrupting Pesticides in Nebraska Groundwater: Trends between Pesticide-contaminated Water and Estrogen-related Cancers in An Ecological Observational Study, *Water*. 13 (2021). <https://doi.org/10.3390/w13060790>.
- [88] E. Pelizzetti, V. Maurino, C. Minero, V. Carlin, M.L. Tosato, E. Pramauro, O. Zerbinati, Photocatalytic degradation of atrazine and other s-triazine herbicides, *Environ. Sci. Technol*. 24 (1990) 1559–1565. <https://doi.org/10.1021/es00080a016>.
- [89] E. Canelli, Chemical, bacteriological, and toxicological properties of cyanuric acid and chlorinated isocyanurates as applied to swimming pool disinfection: a review, *Am J Public Health*. 64 (1974) 155–162. <https://doi.org/10.2105/ajph.64.2.155>.
- [90] L.C. Mahlalela, C. Casado, J. Marugán, S. Septien, T. Ndlovu, L.N. Dlamini, Photocatalytic degradation of atrazine in aqueous solution using hyperbranched polyethyleneimine templated morphologies of BiVO₄ fused with Bi₂O₃, *Journal of Environmental Chemical Engineering*. 8 (2020) 104215. <https://doi.org/10.1016/j.jece.2020.104215>.

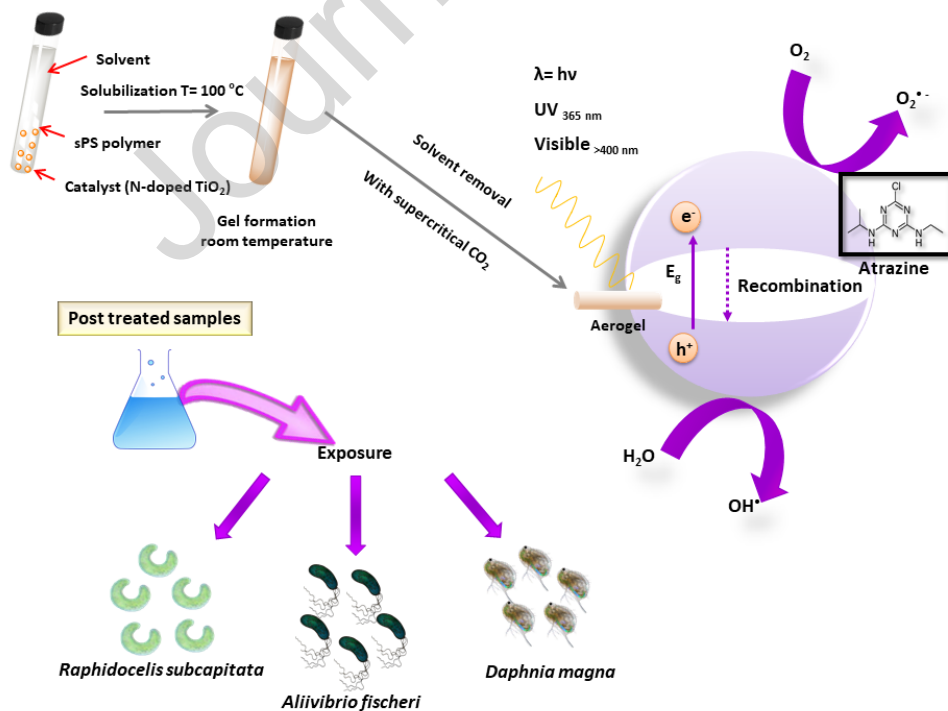
Credit author statement

- Wanda Navarra: Investigation; Formal analysis; Writing - Original Draft;
- Olga Sacco: Conceptualization; Formal analysis; Writing - Original Draft;
- Christophe Daniel: Conceptualization; Validation; Funding acquisition
- Vincenzo Venditto: Conceptualization; Validation; Writing - Original Draft;
- Vincenzo Vaiano: Conceptualization; Validation; Writing - Original Draft;
- Davide Anselmo Luigi Vignati: Ecotoxicological investigation; Resources; Writing - Original Draft;
- Clément Bojic Ecotoxicological investigation; Writing - Original Draft;
- Giovanni Libralato: Supervision; Writing - Review & Editing;
- Giusy Lofrano: Supervision; Writing - Review & Editing;
- Maurizio Carotenuto: Supervision; Writing - Review & Editing; Resources

Declaration of interests

The authors declare that they have no known competing financial interests or personal relationships that could have appeared to influence the work reported in this paper.

Graphical abstract



Highlights

- Effective synergy between NdT and sPS aerogel was observed
- sPS/NdT was always more active in the atrazine degradation than NdT powder
- Degradation kinetic of atrazine was independent from its initial concentration
- Photocatalytic activity of sPS/NdT not decreased after five reusability tests
- After 72 h no or low toxicity was observed under investigated treatments

Journal Pre-proof